Scattering of vibrational waves in perturbed two-dimensional multichannel asymmetric waveguides as on an isolated step

A. Virlouvet
Laboratoire de Physique de l'Etat Condensé, UPRES A 6078, Université du Maine, 72017 Le Mans, France

A. Khater
Laboratoire de Physique de l'Etat Condensé, UPRES A 6078, Université du Maine, 72017 Le Mans, France and SRSIM de CEA/Saclay, 91191 Gif sur Yvette, France

H. Aouchiche and O. Rafil
Département de Physique, Université de Tizi-Ouzu, Tizi-Ouzu, Algeria

K. Maschke
Institut de Physique Appliquée, Ecole Polytechnique Fédérale, CH-1015 Lausanne, Switzerland
(Received 23 April 1997; revised manuscript received 6 February 1998)

We investigate the scattering of vibrational waves at the step interface between two structurally different waveguides, namely, one and two coupled atomic layers occupying the half spaces on either side of the step. The model presented is also instructive for the study of the scattering of surface phonons by random isolated steps in vicinal surfaces. The complexity of the scattering of vibrational waves, in contrast with coherent electron transport, which in part may be attributed to the vector character of the vibrational fields, is further enhanced in the present study owing to the intrinsic asymmetry of the system normal to the step as well as to its two-dimensional extended character. A detailed discussion of the reflection and transmission spectra is presented for the scattering processes in the two possible geometries normal to the step.
[S0163-1829(98)01747-0]

I. INTRODUCTION

Diffraction and localization phenomena in disordered low-dimensional systems have long been of theoretical interest for systems that can yield useful information with well-defined mathematical properties.[1] These systems are now of renewed interest owing to advances in technology that permit the construction of devices at the nanometric scale. Most of the recent research has been oriented towards the study of electronic scattering in quasi-one-dimensional systems, the basic motivation being the need to understand the limitations that structural disorder, or other kinds of disorder, may have on the physical properties of microelectronics devices.

Interest in the understanding of electronic transport phenomena, multiple scattering, and quantum interference in disordered low-dimensional mesoscopic systems has been early.[2–5] In contrast, the study of vibrational phenomena in such systems has not received the attention it deserves, even though scattering in one-dimensional disordered atomic chains,[6] and in quasi-one-dimensional waveguides[7] has been studied.

There are strong similarities between electronic scattering and the scattering of vibrational waves since, mathematically speaking, we just replace the Schrödinger equation by the dynamical equation. The scattering of the vibrational waves is, however, more complicated as one is confronted with the scattering of vector fields instead of scalar fields, as in the electronic case.

Parallel to the interest in low-dimensional disordered mesoscopic systems there is also an increasing interest in the theoretical and experimental study of the dynamics of disordered surfaces.[8–13] The presence of defects on surfaces, as, for example, random steps, is important to their electronic and vibrational properties.

The problem of the dynamics of *periodic* steps in vicinal surfaces has been addressed,[13–15] and in a recent work[16] we present a precursor model for the study of the dynamics of a random *isolated* surface step. In these studies, the vicinal surfaces are treated as effectively low-dimensional systems, with the distinctive feature of a direction either normal to the average periodic surface,[13,14] or, when considering an isolated step,[16] in the direction normal to the step edge. Our results[16] are in qualitative agreement with previous work[15] and demonstrated that the breakdown of translational symmetry normal to the step edge gives rise to several branches parallel to the step, other than the Rayleigh branch on the ordered surface.

In the present paper, we investigate the scattering of vibrational waves on an isolated step in crystallographic waveguides in the harmonic approximation. The monoatomic step is treated as the perturbed interface between two slabs, the first consisting of two coupled atomic layers and the other of a single atomic layer, occupying two half spaces on either side of the step as shown in Fig. 1. The model is quasi-two-dimensional, where the distinctive feature is a direction normal to the step edge. The complexity in the present vibrational study is enhanced, as compared to previous work concerning quasi-one-dimensional waveguides[7] by the need to treat the increased dimensionality. Also, the system of an isolated step edge is a more general case since it

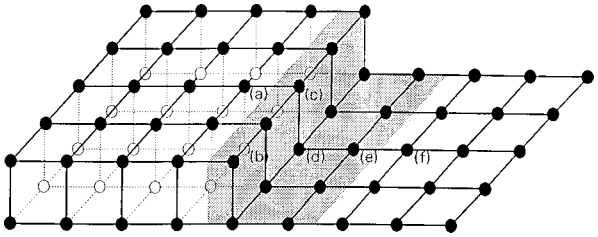

FIG. 1. A schematic representation of an isolated infinite step defect, modeled as the interface between the single atomic layer and the two coupled atomic layers, in two separate half spaces. The system is crystallographically simple square and simple cubic in the two half spaces, respectively.

consists of two structurally different waveguides leading to an intrinsic asymmetry between the two distinct half spaces on either side of the interface step. The model that is presented is consequently also instructive for the study of the scattering of surface phonons by random isolated steps in vicinal surfaces.

In Sec. II, we present the dynamics and propagating characteristics of the two perfect waveguides in the half spaces to the left and right of the monoatomic step, introducing the essential features of the formalism we need later on. Section III presents the algebraic formalism for scattering at an isolated defect and in particular at the isolated infinite step. In Sec. IV, we give typical examples for the scattering of waves in the two asymmetric geometries, for waves incoming at different angles of incidence with respect to the step edge, from the simple plane onto the double plane and in the opposite sense.

II. THE ISOLATED STEP HALF SPACES

A. Propagating modes

Our structural model is based on two coupled semi-infinite atomic layers interfacing with a single semi-infinite atomic layer, as shown in Fig. 1, with nearest- and next-nearest-neighbor interactions. These interactions are considered as the same in both half spaces of the system without loss of generality, letting r denote their ratio. Moreover, we allow for a modification of the strain field in the step region by the parameter λ, which denotes the ratio of these modified force constants to the constants of the system outside the step region. The step region is defined as the gray area in Fig. 1. For simplicity, we take the same distance **a** between adjacent masses in the different Cartesian directions x,y,z.

The matching method[17] that we employ in this paper has previously been extended to study wave scattering by isolated defects in quasi-one-dimensional disordered mesoscopic systems.[6,7] The matching method allows one to deal with both aspects of localized modes and of scattering of waves at defects within the same mathematical framework.

The equation of motion of an atom $\boldsymbol{l}$ at the variable frequency ω is given as usual in the harmonic approximation[18] by

$$\omega^2 m(l) u_\alpha(l,\omega) = -\sum_{l' \neq 1} \sum_{\beta} K(l,l') \left(\frac{r_\alpha r_\beta}{d^2} \right) \times [u_\beta(l,\omega) - u_\beta(l',\omega)], \qquad (1)$$

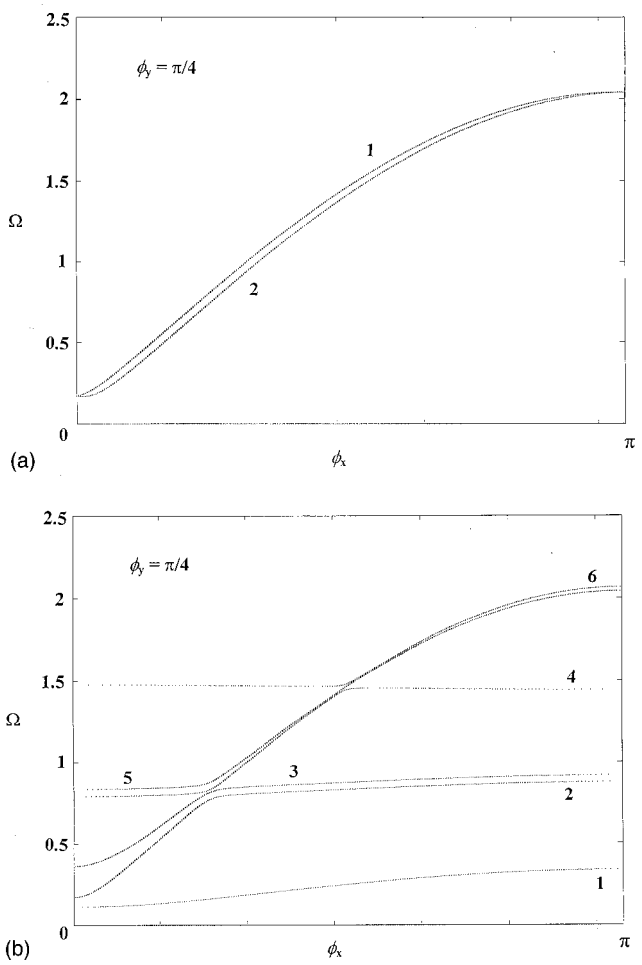

FIG. 2. (a) The dispersion branches for the propagating modes or phonons for the single atomic layer ($p1$) with ϕ_x running over the Brillouin zone $[0,\pi]$, for the case of $\phi_y = \pi/4$. (b) The dispersion branches for the propagating modes or phonons for the coupled atomic layers ($p2$), with ϕ_x running over the Brillouin zone $[0,\pi]$, for the case of $\phi_y = \pi/4$.

for $(\alpha,\beta) \in \{x,y,z\}$, where $m \equiv m(\boldsymbol{l})$ is the atomic mass for sites $\boldsymbol{l}$, $u_\alpha(\boldsymbol{l},\omega)$ is the displacement field along the α direction, r_α the corresponding cartesian component of the radius vector between atoms $\boldsymbol{l}$ and $\boldsymbol{l}'$, d is the distance $\boldsymbol{l}\boldsymbol{l}'$, and $K(\boldsymbol{l},\boldsymbol{l}')$ is the force constant between $\boldsymbol{l}$ and $\boldsymbol{l}'$. In this representation the x and y axes are taken, respectively, normal and parallel to the infinite step edge in Fig. 1. The z axis, not to be confused with the phase factors introduced later, is normal to the plane of the x and y axes.

The dynamics of propagating modes is described by the traveling wave solutions of Eq. (1) in each half space. Typical results are presented in Fig. 2 as a function of the wave vectors (ϕ_x, ϕ_y), where $\phi_x = \mathbf{a}k_x$, **a** is the interatomic distance and k_x is the one-dimensional reciprocal lattice wave vector in the direction normal to the step edge.

In Figs. 2(a) and 2(b), the bulk waveguide phonons are presented for $\phi_y = \pi/4$, for the single atomic layer and the two coupled atomic layers, respectively. The quantity $\phi_y = \mathbf{a}k_y$, where k_y is the one-dimensional reciprocal lattice wave vector in the direction parallel to the step edge. Figure 2(a) illustrates the propagating modes for the single atomic layer, and Fig. 2(b) for the two coupled atomic layers. The

quantities (ϕ_x,ϕ_y) determine the angle of incidence of the incoming wave with respect to the step edge. Ω is the dimensionless frequency given by $\Omega^2=\omega^2/\omega_0^2$, where ω_0 is a characteristic lattice frequency given by $\omega_0^2=K(l,l')/m$, for l and l' as nearest neighbors.

The propagating modes in Fig. 2(a) are two branches that correspond to different polarizations. Mode 1 corresponds to polarizations for the atomic movements that are in phase along the x and y directions in the atomic plane, whereas mode 2 corresponds to polarizations out of phase along these directions.

In Fig. 2(b), we have six modes. The polarization of mode 1 is slightly different from the other modes, it is along the z direction, the movements of the coupled atoms in the two atomic planes being in phase. Modes 3 and 5 are predominantly polarized along the x direction normal to the step, the atoms on the two atomic planes being out of phase. Modes 2, 4, and 6 are predominantly polarized along the x direction, the atoms on the planes being in phase. It is noted that the total frequency ranges Ω for the groups of modes (3,5) and (2,4,6) are approximately the same and fall in the range $[\sim 0.25,\sim 2.1]$. These polarizations are typical for other values of ϕ_y.

B. Evanescent modes

The evanescent vibrational fields in the single atomic layer and in the two coupled layers, away from the step region, are described, respectively, by the phase factor doublets $(z'(i),z'(i)^{-1})$ and $(z(j),z(j)^{-1})$, going from one site to its nearest neighbors or vice versa along the direction normal to the step edge. Here, i and j label the solutions in the semi-infinite single (two coupled) atomic layers. The evanescent vibrational fields in each half space are given by the evanescent solutions of the equations of motion, determined by the conditions that $|z'(i)|<1$ and $|z(j)|<1$, respectively.

Using Eq. (1), the atomic motion on a site $(n_x n_y)$ outside the step region, in the single atomic layer, can be expressed as

$$[\Omega^2\boldsymbol{I}-N(\phi_y,z',r,\lambda)]|u'\rangle=|0\rangle. \tag{2}$$

A similar set of equations is obtained for the two coupled atomic layers for the sites $(n_x n_y n_z)$, where n_z takes on two different values n_z and n_{z-1} for the two distinct inequivalent atomic layers, as

$$[\Omega^2\boldsymbol{I}-M(\phi_y,z,r,\lambda)]|u\rangle=|0\rangle. \tag{3}$$

The detailed expressions of the dynamical matrices as a function of ϕ_y, r, λ, and z (z') are given in the Appendix.

The nontrivial solutions for the matrices in Eqs. (2) and (3), require that the determinants, $\det[\Omega^2\boldsymbol{I}-N(\phi_y,z',r,\lambda)]$ and $\det[\Omega^2\boldsymbol{I}-M(\phi_y,z,r,\lambda)]$, vanish. This gives rise to two characteristic secular equations in each half space, of 12 degrees in z and four in z', respectively, that may be expressed in the polynomial form as

$$A_0+A_1z+A_2z^2+A_3z^3+A_4z^4+A_5z^5+A_6z^6 +A_7z^7+A_8z^8+A_9z^9+A_{10}z^{10}+A_{11}z^{11}+A_{12}z^{12}=0, \tag{4}$$

$$A_0'+A_1'z'+A_2'z'^2+A_3'z'^3+A_4'z'^4=0, \tag{5}$$

where the coefficients A_n and A_n' are functions of Ω, ϕ_y, r, and λ. Both phase factor doublets z, z^{-1} and z', z'^{-1} can be shown to verify symmetrically the polynomials, owing to the Hermitian nature of the bulk dynamics or reversal time symmetry.[17,19] To satisfy the evanescent conditions $|z|<1$ and $|z'|<1$, however, only six physically acceptable solutions for z and two for z', are retained from the roots of Eqs. (4) and (5). Together these constitute in the space $\{\Omega,\phi_y\}$, the set of evanescent modes $\{z(i),z'(j)\}$, $i\in\{1,2\}$ and $j\in\{1,2,3,4,5,6\}$. The evanescent fields are then rigorously determined in the two waveguides each in its half space. Another alternative and equally elegant procedure to calculate these factors has been proposed in Ref. 7.

The solutions of Eqs. (4) and (5) when $|z'(i)|=1$ and $|z(j)|=1$ correspond effectively to propagating waves in the bulk of the two half spaces that are described by real wave vectors. Both propagating and evanescent solutions are needed to describe the scattering solutions in the presence of defects such as the isolated step.

III. SCATTERING AT THE STEP

Since the perfect semi-infinite layers do not couple between different eigenmodes they may be considered as perfect waveguides, and we can treat the scattering problem for each eigenmode separately. Consider, for example, the case of an incoming propagating wave i, where $|z'(i)|=1$, incident from the single atomic plane $(p1)$ onto the step in the direction of the double atomic planes $(p2)$. The resulting scattered waves, due to the *elastic* scattering at the isolated step, are composed of reflected and transmitted parts, which gives rise to vibrational fields in both half spaces. The Cartesian components α of the displacement field for an atom outside the step region, i.e., outside the gray area of Fig. 1, can then be expressed using the matching approach.[17,19,7] For an atomic site in the single atomic layer as the sum of the incident wave and a superposition of the eigenmodes of the perfect simple square waveguide, at the same frequency

$$u'_\alpha(n_x n_y)=A'(\alpha,i)[z'(i)]^{-n_x} +\sum_{i'=1}^{2}[z'(i')]^{n_x}R^{+}_{ii'}(p1/p2)A'(\alpha,i'). \tag{6}$$

For an atomic site in the coupled layers, this is given as

$$u_\alpha(n_x n_y n_z)=\sum_{j=1}^{6}[z(j)]^{-n_x}R^{-}_{ij}(p1/p2)A(\alpha,j,n_z). \tag{7}$$

The quantities $R^{+}_{ii'}(p1/p2)$ denote, for the present case, the reflection coefficients for scattering elastically the given incident wave i into the $i'=1,2$ eigenmodes of the $(p1)$ half space, at the same frequency. Similarly, $R^{-}_{ij}(p1/p2)$ are the transmission coefficients due to this incident wave into the $j=1,2,\ldots,6$ eigenmodes of the $(p2)$ half space. The coefficients $A(\alpha,j,n_z)$ and $A'(\alpha,i')$, denote the relative weighting factors, or polarizations, associated to the different atomic displacements u_α and u'_α on their sites in the two half spaces[17,19,7] at the frequency of the scattering process.

Let $|R\rangle$ denote the basis vector for the reflection and transmission coefficients in a constructed space, and $|U\rangle$ that

composed by the displacements of a set of irreducible atomic sites in the step region considered as an infinite defect. The equations of motion for the step, coupled to the rest of the system, can then be rewritten in terms of the vector $[|U\rangle,|R\rangle]$.

The necessary minimum set of sites defining the vector $|U\rangle$ are indicated in Fig. 1 by the letters (c), (d), (e), in virtue of the high-symmetry direction along the direction of the step. Taking (d) as the origin, their coordinates are as follows: (c) $=(0,0,+1)$, (d) $=(0,0,0)$, (e) $=(+1,0,0)$. Using the transformations connecting the displacement fields in Eqs. (3), (6), and (7), we obtain a square linear *inhomogeneous* system of equations of the form

$$[\Omega^2 I - D(\phi_y, r, \lambda, z(j), z'(i))][|U\rangle,|R\rangle] = -|IH\rangle, \quad (8)$$

where the vector $-|IH\rangle$, mapped appropriately onto the basis vectors, regroups the inhomogeneous terms describing the incoming wave.

Note that all the sites in the step region have three degrees of freedom for their atomic displacements, since we allow for next-nearest-neighbor interactions between the $(n_x n_y n_z)$ sites on the step edge of the two coupled atomic layers with the sites $(n_x n_y)$ of the single atomic layer, in this region. The size of the vector $|U\rangle$ depends on the minimum set of atomic sites above that is necessary for a description of the perturbed step region. The dimensions of the matrix Eq. (8) depends on this and on the size of $|R\rangle$.

The solutions of Eq. (8) yield the displacements $|U\rangle$ of the irreducible set of atomic sites in the step region, as well as the reflection and transmission coefficients $R^+_{ii'}(p1/p2)$ and $R^-_{ij}(p1/p2)$ at the scattering frequency Ω, which determine the Cartesian displacements of the atoms in the unperturbed regions of the two half spaces away from the perturbed step region.

The scattering behavior is usually described in terms of the scattering matrix, whose elements are given by the relative reflection and transmission amplitudes $r_{ii'}(p1/p2)$ and $t_{ij}(p1/p2)$, at the scattering frequency Ω. In order to obtain unitarity of the scattering matrix, the scattered waves have to be normalized with respect to their group velocity.

In the following we concentrate on the discussion of the reflection and transmission probabilities for a wave incident from the $(p1)$ half space onto the step in the direction of $(p2)$ half space. They are given by the absolute squares of the respective matrix elements of the scattering matrix. Explicitly, for waves incoming in the eigenmode i from the $(p1)$ half space, the relative reflection amplitudes are

$$r_{ii'}(p1/p2) = \frac{v_{i'}}{v_i}|R^+_{ii'}(p1/p2)|^2 \quad (9)$$

and the relative transmission amplitudes

$$t_{ij}(p1/p2) = \frac{v_j}{v_i}|R^-_{ij}(p1/p2)|^2. \quad (10)$$

Note that v_s is the group velocity of the eigenmode s, which is put equal to zero for evanescent modes in the two waveguides.

The evanescent modes are necessary for a complete description of the overall dynamics and of the scattering amplitudes of the multichannel waveguides, although they do not contribute to energy transfer.

We can further define reflection and transmission probabilities for a given eigenmode at the scattering frequency Ω, by the following expressions:

$$r_i = \sum_{i'} r_{ii'}(p1/p2), \quad (11)$$

$$t_i = \sum_{j} t_{ij}(p1/p2). \quad (12)$$

In order to describe the overall transmission of mesoscopic disordered multichannel systems at a given frequency Ω, it is useful to define a total transmission probability $\sigma(\Omega)$ by

$$\sigma(\Omega; p1/p2) = \sum_{i,j} t_{ij}(p1/p2), \quad (13)$$

where the sum is carried out over all propagating modes at the frequency Ω. The transmission probabilities $t_i(\Omega)$ per eigenmode i, and the total transmission probability $\sigma(\Omega; p1/p2)$, are important for calculating experimentally measurable quantities.

The case of a propagating wave incident from the half space $(p2)$ onto the step in the direction of the half space $(p1)$ can be treated in a similar manner. Again, the elastic scattering at the isolated step gives rise to vibrational fields in both half spaces. The analysis, however, is somewhat more complicated in this geometry because of the multiplicity of eigenmodes in the double-plane half-space $(p2)$ waveguide. The notations for the relative reflection and transmission amplitudes, and the reflection and transmission probabilities per eigenmode, for this geometry rest unchanged except for replacing $p1/p2$ wherever it occurs by $p2/p1$, and arranging the indices i, i', j, j' correctly with respect to the reflection and transmission coefficients R^+ and R^-, for each eigenmode diffraction study.

The interference phenomena discussed in this paper are derived from the dynamical equations in the harmonic approximation, which can be applied to any length scale, provided that the phase coherence is not destroyed by dissipative effects. The results presented apply, hence, equally to defect induced effects in macroscopic two-dimensional systems. This provides a mean at the macroscopic scale of balls and springs, by which one can definitely probe the transmission resonances.

IV. RESULTS AND DISCUSSION

The functional behaviors of the different modes may be presented in the z and z' planes by the curves $\Omega(z)$ and $\Omega(z')$, on and inside the unit circle. These become very intricate even for only two modes.[7] In the present paper, we have eight modes to follow in the complex plane and it is not convenient to present them graphically.

For our numerical calculations presented below we have chosen $r = 0.05$, considering that next-nearest-neighbor interactions to be much weaker than the nearest-neighbor ones, and $\lambda = 1.05$, which accounts for the relative hardening of

the force constants in the step region. Clearly, the details of the force constants do not matter in this numerical calculation used to illustrate qualitative trends and results for phonon transport. The same type of resonances we consider and wish to draw attention to in this numerical calculation will arise whatever the choice of the force constants.

The dynamics of propagating modes is described by the traveling wave solutions of Eq. (1) in each half space. The results presented in Fig. 2 as a function of the wave vector $\phi_x = \mathbf{a}k_x$, where k_x is the one-dimensional reciprocal lattice wave vector in the direction normal to the step edge have been briefly discussed already in Sec. II. In Figs. 2(a) and 2(b) the bulk waveguide dispersion branches $\Omega(\phi_x)$, are presented for both the single atomic layer and the two coupled atomic layers, for the dimensionless wave vectors $\phi_y = ak_y = \pi/4$, where k_y is the one-dimensional reciprocal lattice wave vector in the direction parallel to the step edge.

The propagating modes in Fig. 2(a) are two branches that correspond to polarizations for the atomic movements that are in phase and out of phase along the x and y directions in the atomic plane, respectively.

The six modes in Fig. 2(b) correspond to essentially three types of polarizations. Mode 1, slightly different from the other modes, is polarized along the z direction, the movements of two coupled atoms in different layers being in phase. Modes 3 and 5 are predominantly polarized along the x direction normal to the step, the atoms on the two atomic planes being out of phase. Modes 2, 4, and 6 are predominantly polarized along the x direction, the atoms on the planes being in phase. The total frequency ranges along Ω for the groups of modes (3,5) and (2,4,6) for the two coupled atomic layers are approximately the same, falling in the range $[\sim 0.25, \sim 2.1]$.

Note for example, in Fig. 2(a) that the two branches 1 and 2 for the single atomic layer are degenerate for $\phi_x = 0$ and π at the Brillouin-zone boundaries, which turns out to be the case for all values of ϕ_y. Note also the existence around $\Omega = 1.5$ of a dispersionless ''mode'' for the two coupled atomic layers, which interacts only weakly with the crossing optical branches of the two different branches.

The systems of Eqs. (4) and (5) may be solved for wavelike propagating solutions, which gives the phonon bulk band limits for the single atomic layer denoted by the curves $p1$, and those for the two coupled atomic layers denoted by the curves $p2$, respectively, in Fig. 3. We note the presence of a small and thin window in the bulk continuum, which becomes larger when r increases. Note that the $p2$ continuum is similar to the projection of bulk phonon bands for an fcc crystal on a Miller low-index surface. This similitude may be made stronger by adjusting appropriately the value of r, and illustrates the usefulness of a low-dimensional approach for this kind of surface problem.

Knowledge of the modes that are localized on the isolated infinite step and that propagate parallel to the step edge is important in principle for a complete description of the scattering of waves on the step edge. The dispersion Rayleigh-like branches of these phonon modes are given in Fig. 3 as the curves R_1 and R_2, lying as they should outside the continuum of both half spaces. These branches, which may be made to appear and to disappear as a function of the numerical values attributed to r and λ, arise due to the breakdown of

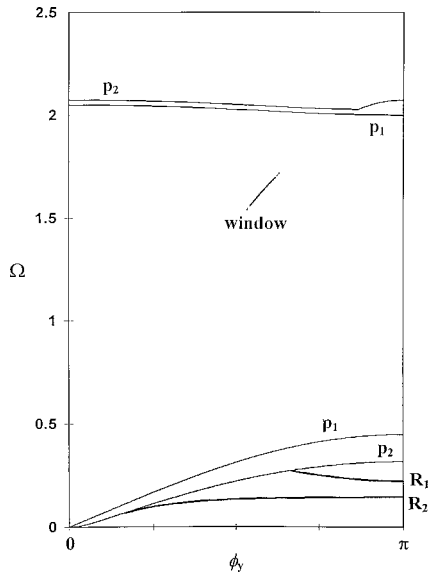

FIG. 3. The Rayleigh step localized dispersion branches R_1, R_2 as a function of the wave vector ϕ_y in the direction of high symmetry of the system along the step edge $p1$ and $p2$ denote the bulk continuum phonon band limits for the single and coupled two atomic layers, respectively.

translational symmetry in the direction normal to the step. The branches R_1 and R_2 are in qualitative agreement with the theoretical results of Ref. 14, although a detailed comparison shows that the nature of the modes is not the same in the two studies. In the cited work the authors label two of the branches as primary and secondary Rayleigh modes, the secondary being a backfolded excitation owing to the *periodicity* of their vicinal surface. In our case there is no such folding, rather the $R1$ and $R2$ branches arise because the *isolated* monoatomic step provokes the breakdown of translational symmetry normal to the step edge, and thus gives rise to new branches propagating parallel to yet localized normal to the step.[16]

A. Scattering of waves incident from the single-plane waveguide

In this section we present some results for the case of the scattering of an incoming propagation eigenmode wave i, where $|z'(i)| = 1$, and i can be 1 and 2, incident from the singlet atomic plane $(p1)$ onto the step in the direction of the double atomic planes $(p2)$.

Numerical results may be obtained for a variety of ϕ_y values. We have investigated the evolution of these results and found that it is relatively smooth for scattering studies from $\phi_y = 0$ to $\phi_y = \pi$.

In Fig. 4(a) we present the relative reflection and transmission amplitudes r_{11} and r_{12} as a function of the scattering frequency Ω, for the guided mode $i = 1$ indicated in Fig. 2, when this is incident from the single plane onto the double plane with a $\phi_y = \pi/4$ component. Note that these reflection amplitudes span the whole range of frequencies of the given branch, beginning at $\phi_x = 0$ and ending at $\phi_x = \pi$. Since the two branches 1 and 2 in this case are degenerate at these

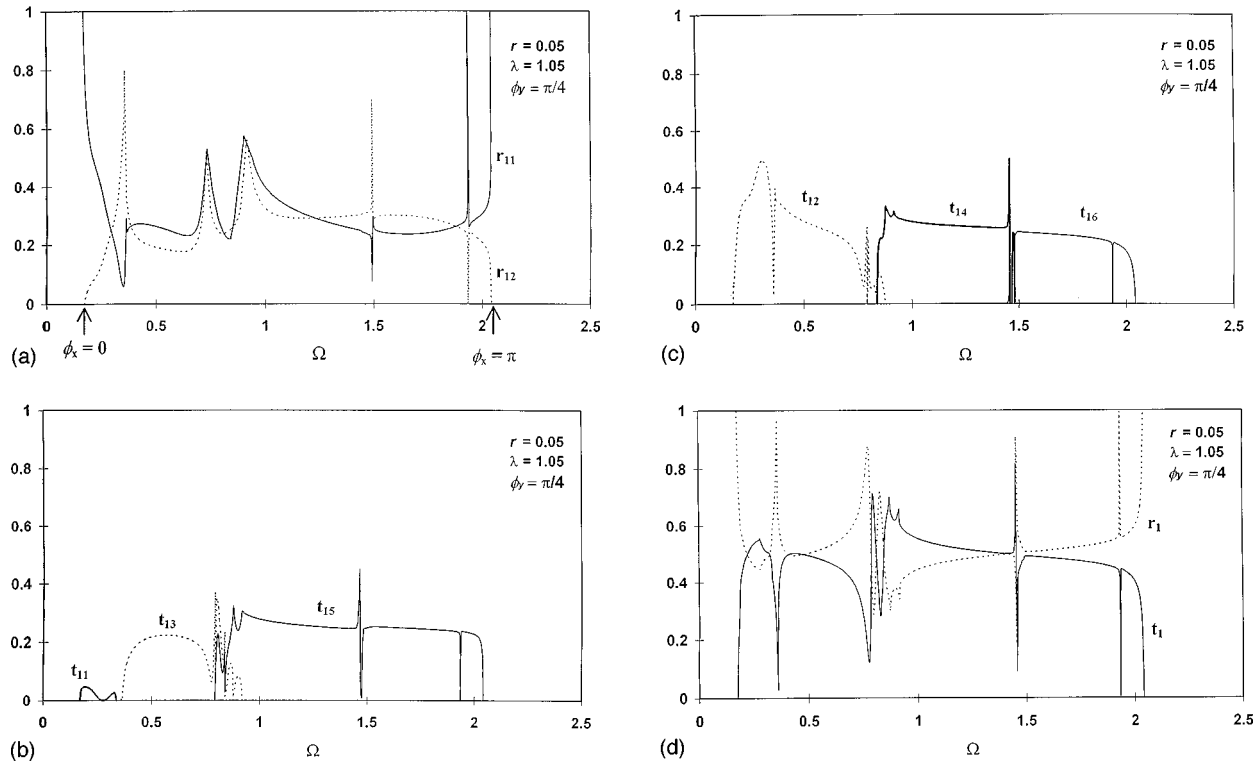

FIG. 4. (a) The relative reflection amplitudes r_{11} and r_{12} into the single layer modes 1 and 2, due to the scattering at the step defect of the single layer mode 1 wave; the case of $\phi_y=\pi/4$. (b) The relative transmission probabilities t_{11}, t_{13}, and t_{15} into the coupled layers modes 1, 3, and 5, due to the scattering at the step defect of the single layer mode 1 wave; the case of $\phi_y=\pi/4$. (c) The relative transmission amplitudes t_{12}, t_{14}, and t_{16} into the coupled layers modes 2, 4, and 6, due to the scattering at the step defect of the single layer mode 1 wave; the case of $\phi_y=\pi/4$. (d) The partial reflection r_1, and transmission t_1, probabilities, associated to the scattering at the step defect of the single layer mode 1 wave; the case of $\phi_y=\pi/4$.

points in the reciprocal space, they are also completely out of phase, which explains why r_{11} and r_{12} at the corresponding frequencies are at antipodes as in Fig. 4(a). It is likely that the Rayleigh-like localized mode $R1$ embedded in the continuum couples to this scattering process giving rise to a resonance structure near the frequency $\Omega=0.4$. Note that the evanescent eigenmodes *normal* to the step edge, which characterize the displacement field of the Rayleigh-like modes themselves propagating *parallel* to the step edge, do contribute intrinsically under Eqs. (6) and (7) towards the complete description of the scattering process.

These relative reflection amplitudes register, as is observed in Fig. 4(a), rapid variations in the range of frequencies $0<\Omega<0.5$, which corresponds to the onset of nonzero relative transmission amplitudes $t_{1j}(\Omega)$ via the waveguide mode branches $j=1,3,5$ and $j=2,4$ of the double atomic plane half space, as may be observed in Figs. 4(b) and 4(c), respectively. The onset and the disappearance of the transmission amplitudes correspond to the frequency range of the existence of these guided modes as propagating waves, as may be shown with reference to Fig. 2(a).

Further, these reflection amplitudes, as well as the corresponding transmission amplitudes, as may be seen in Figs. 4(c) and 4(d), show important resonance variations around the frequencies $\Omega=0.8$ and 1.5. These resonances may be interpreted as due to the coupling with the dispersionless ''modes,'' which appear in Fig. 2(a) near these frequencies and describe the flat parts of the branches $j=2,3,5$ and 4,6 in the two coupled atomic layers half space. They also show coupling to the embedded $R1$ mode near $\Omega=0.4$. The ensemble of these resonances are recurrent in Figs. 6(a)–6(d).

The resonance in the range $1.911<\Omega<1.945$, which appears for the relative transmission amplitudes t_{15} and t_{16} as well as in the relative reflection amplitudes, at a peak of $\Omega=1.935$, has the features of a Fano resonance, i.e., its presence indicates coupling with a resonant defect state embedded in the continuum.

In Fig. 4(d) we present the reflection and transmission probabilities r_1 and t_1 as a function of the frequency Ω. These are obtained from Eqs. (11) and (12). The sum of both is unity for all frequencies, as is required from the *unitarity* condition.

In Figs. 5(a) and 5(b), we illustrate the scattering study for $\phi_y=\pi$. We note in particular the disappearance of the coupling to certain eigenmodes in the double plane $(p2)$ due to the shifting of the modes in this waveguide. A particular feature is the absence of the resonance in the transmission and reflection spectra at the peak frequency $\Omega=1.935$, for ϕ_y values other than $\pi/4$, which must be due to symmetry considerations.

Results for scattering from the eigenmode branch $i=2$, may be also obtained in a similar manner. The relative amplitudes for scattering from the modes $i=2$ are fairly similar to those for scattering from $i=1$. We have checked the resonance at the peak frequency $\Omega=1.935$ when scattering from

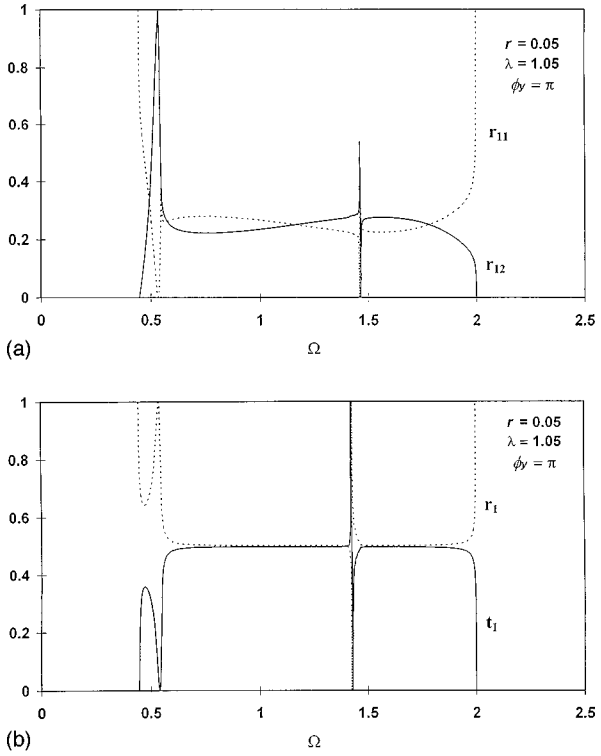

FIG. 5. (a) The same as in Fig. 4(a) for the case of $\phi_y = \pi$. (b) The same as in Fig. 4(d) for the case of $\phi_y = \pi$.

the $i=1$ and 2 modes, for different values of ϕ_y. This resonance seems to exist only for $\phi_y \approx \pi/4$.

B. Scattering of waves incident from the double-plane waveguide

In this section, we present some results for an incoming propagating eigenmode wave j, incident from the double atomic planes $(p2)$ onto the step in the direction of the single atomic plane $(p1)$. Here $|z(j)|=1$, and j can be any one out of the six available modes $j=1,2,3,4,5,6$ in the $(p2)$ double atomic planes.

In this case there are six modes that can contribute. In order to illustrate this we present our results in Fig. 6 for the $j=2$ mode, i.e., for the relative reflection and transmission amplitudes $r_{2j'}(p2/p1)$ and $t_{2i}(p2/p1)$, and for the reflection $r_2=\Sigma_{j'} r_{2j'}(p2/p1)$, and transmission $t_2=\Sigma_i t_{2i}(p1/p2)$ probabilities, as a function of the scattering frequency Ω.

In Figs. 7(a)–7(e), we present the total transmission probabilities $\sigma(\Omega;p1/p2)$ for waves incident from the $(p1)$ onto the $(p2)$ half spaces for, respectively, $\phi_y=0$, $\pi/4$, $\pi/2$, $3\pi/4$, π. The total transmission probabilities for waves incident from the $(p2)$ onto the $(p1)$ half spaces are given in Figs. 8(a) and 8(b) for just $\phi_y=\pi/4$ and π, to limit the number of figures. These two latter results are, however, sufficient to illustrate the differences between the total transmission probabilities in the two geometries. In both sets of Figs. 7 and 8, the dashed histograms represent the total hypothetical pho-

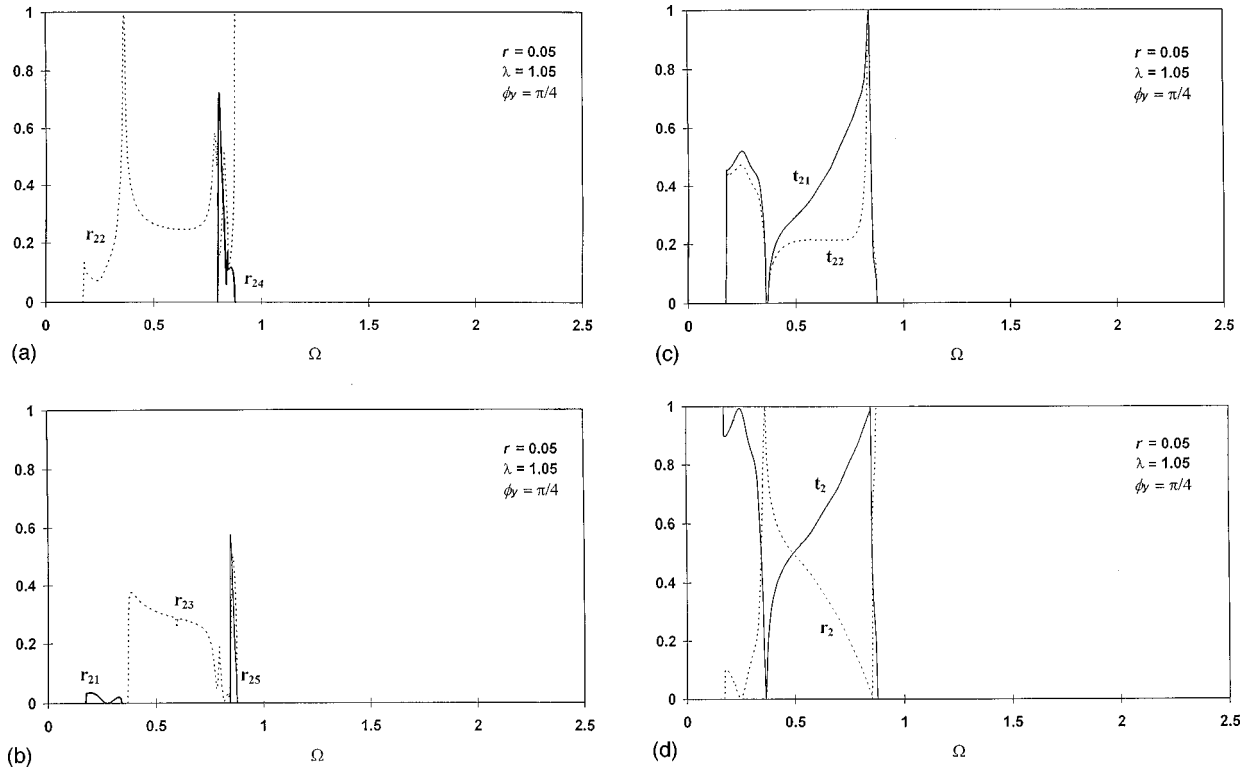

FIG. 6. (a) The relative reflection probabilities r_{22} and r_{24} into the coupled layers modes 2 and 4, due to the scattering at the step defect of the coupled layers mode 2 wave; the case of $\phi_y=\pi/4$. (b) The relative reflection amplitudes r_{21}, r_{23}, and r_{25} into modes 1, 3, and 5 of the coupled layers, due to the scattering at the step defect of the coupled layers mode 2 wave; the case of $\phi_y=\pi/4$. (c) The relative transmission amplitudes t_{21} and t_{22} into the single layer modes 1 and 2 due to the scattering at the step defect of the coupled layers mode 2; the case of $\phi_y=\pi/4$. (d) The partial reflection r_2, and transmission t_2, probabilities, associated to the scattering at the step defect of the coupled layers mode 2 wave; the case for $\phi_y=\pi/4$.

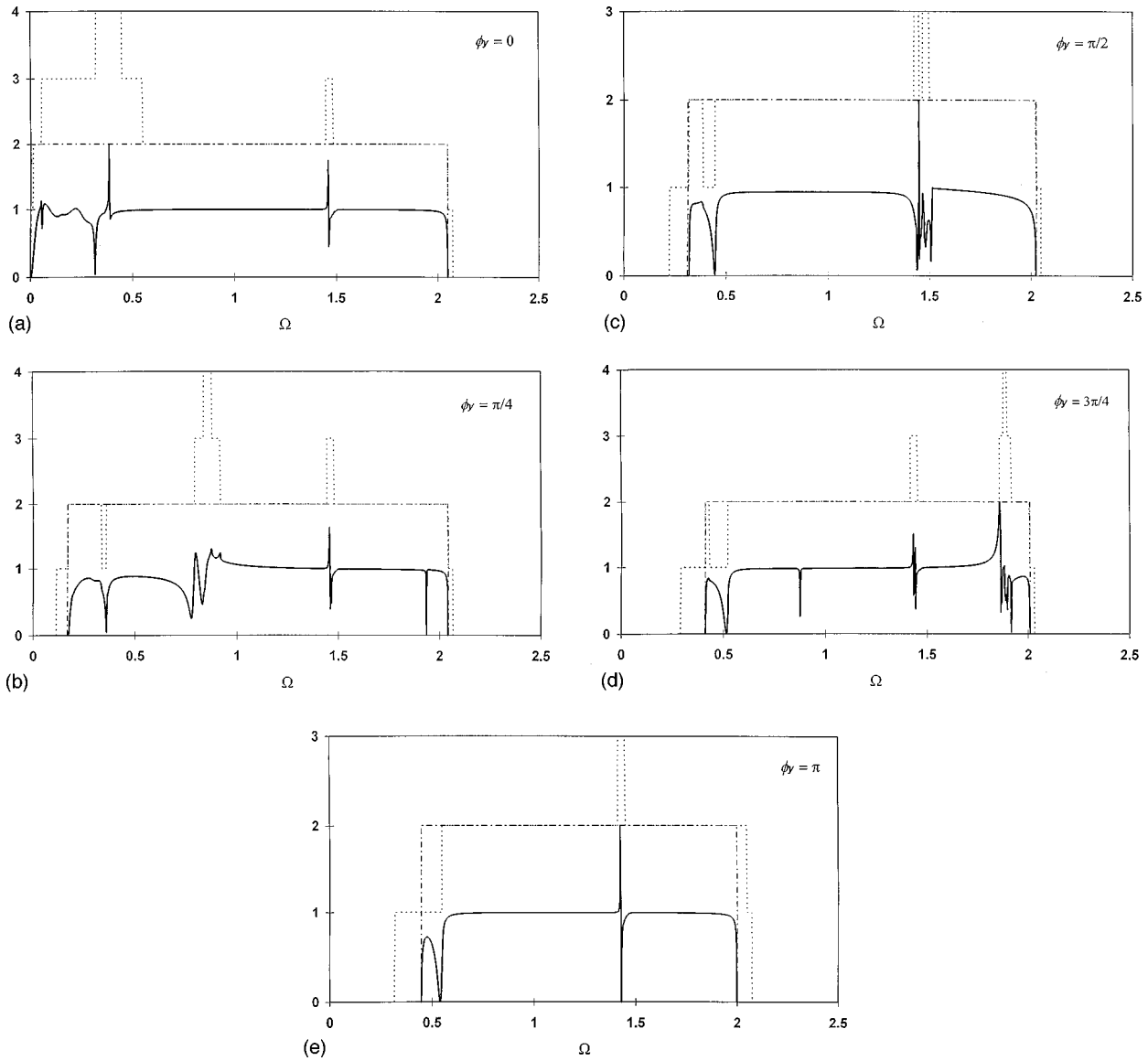

FIG. 7. (a) The total transmission probability from the single layer into the two coupled layers due to the scattering at the step defect of the single layer waves. The dashed histogram represents the total hypothetical phonon transmission capacity for the two coupled layers, and the dashed and dotted histogram that for the single layer. These results are for case of $\phi_y = 0$. (b) As in (a) for the case of $\phi_y = \pi/4$. (c) As in (a) for the case of $\phi_y = \pi/2$. (d) As in (a) for the case of $\phi_y = 3\pi/4$. (e) As in (a) for the case of $\phi_y = \pi$.

non transmission capacity for the two coupled layers, and the dashed and dotted histograms those for the single layer, at the frequencies of interest and for a given choice of the ϕ_y component. The resonances due to coupling of incoming waves to the step defect induced states embedded in the continuum may be observed in Figs. 7 and 8, as illustrated in previous figures.

V. CONCLUSIONS

In the present paper we have developed an approach that allows us to treat the scattering of vibrational waves in perturbed multichannel two-dimensional systems in an efficient manner by solving the dynamical equations directly for scattering boundary conditions. It should be emphasized that the case of vibrational waves, which has not yet been sufficiently treated in the literature for such systems, is more complicated than the electron case, the essential difference being that the wave functions in the Schrödinger equation are complex *scalars*, whereas the vibrational amplitudes are complex *vectors*. Our present work provides a basis study of interference phenomena involving polarizable vector waves in two-dimensional waveguides.

The algebraic approach presented in this paper can be generalized in principle to the scattering of vibrational waves in two-dimensional infinite structures with defects that break the symmetry in two-dimensional space, based on the precedent work[11] that generalizes the matching procedure to such systems.

Our numerical results in this study show that in spite of their different character, the scattering of vibrational waves has some features in common with the scattering of electron waves, and can be described in terms of basically the same interference phenomena, namely Fabry-Pérot oscillations and Fano-like resonances. Fabry-Pérot oscillations are due to the interference between multiply reflected waves in the per-

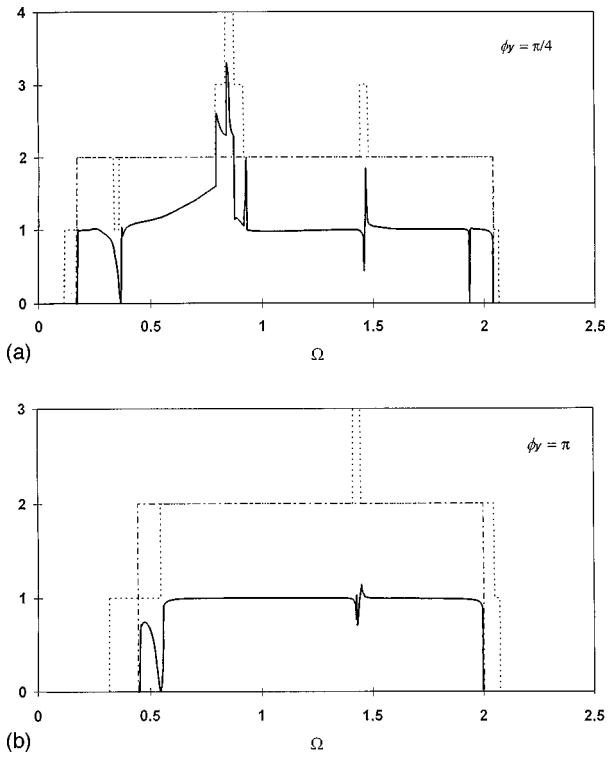

FIG. 8. (a) The total transmission probability from the coupled layers into the single layer due to the scattering at the step defect of the coupled layers waves. The dashed histogram represents the total hypothetical phonon transmission capacity for the two coupled layers, and the dashed and dotted histogram that for the single layer. These results are for case of $\phi_y = \pi/4$. (b) As in (a) for the case of $\phi_y = \pi$.

turbed region; they are relatively absent in this work. Fano resonances appear in the spectra and are usually evoked to describe the interference between propagating transmitted modes and local step-edge defect modes that are embedded in the continuum. The transmission spectra in two-dimensional systems can thus be regarded as fingerprints of their specific defect structure, and may therefore be used for their characterization.

It should be noted that the interference phenomena discussed in this paper are derived from the dynamical equations in the harmonic approximation, which can be applied to any lengthscale provided that the phase coherence is not destroyed by dissipative effects. The results presented apply, hence, equally to defect induced effects in macroscopic two-dimensional systems.

APPENDIX

The equations of atomic motion on the site $(n_x n_y)$ in the bulk of the monoatomic layer can be expressed by

$$[\Omega^2 \boldsymbol{I} - N(\phi_y, z', r, \lambda)]|u'\rangle = |0\rangle \tag{A1}$$

with

$$|u'\rangle = \begin{pmatrix} U'_x(n_x, n_y) \\ U'_y(n_x, n_y) \end{pmatrix} \tag{A2}$$

and

$$[N] = \begin{pmatrix} N(1) & N(3) \\ N(3) & N(2) \end{pmatrix}, \tag{A3}$$

where

$$\begin{aligned} N(1) &= \Omega^2 + (z' + z'^{-1})(1 + r\cos\phi_y) - 2r - 2, \\ N(2) &= \Omega^2 + \cos\phi_y[2 + r(z' + z'^{-1})] - 2r - 2, \\ N(3) &= ir\sin\phi_y(z' - z'^{-1}). \end{aligned} \tag{A4}$$

The equations of atomic motion on the sites $(n_x n_y n_z)$ in the bulk of the two coupled atomic layers can also be expressed in a resumed form as

$$[\Omega^2 \boldsymbol{I} - M(\phi_y, z, r, \lambda)]|u\rangle = |0\rangle \tag{A5}$$

with

$$|u\rangle = \begin{pmatrix} U_x(n_x, n_y, n_z) \\ U_y(n_x, n_y, n_z) \\ U_z(n_x, n_y, n_z) \\ U_x(n_x, n_y, n_{z-1}) \\ U_y(n_x, n_y, n_{z-1}) \\ U_z(n_x, n_y, n_{z-1}) \end{pmatrix} \tag{A6}$$

and

$$[M] = \begin{pmatrix} M(1) & M(4) & 0 & M(5) & 0 & M(6) \\ M(4) & M(2) & 0 & 0 & M(7) & M(8) \\ 0 & 0 & M(3) & M(6) & M(8) & M(9) \\ M(5) & 0 & -M(6) & M(1) & M(4) & 0 \\ 0 & M(7) & -M(8) & M(4) & M(2) & 0 \\ -M(6) & -M(8) & M(9) & 0 & 0 & M(3) \end{pmatrix}, \tag{A7}$$

where

$$
\begin{aligned}
M(1) &= -(z+z^{-1})(1+r\cos\phi_y)+2+3r, \\
M(2) &= -\cos\phi_y[2+r(z+z^{-1})]+2+3r, \\
M(3) &= 2r+1, \\
M(4) &= i(z-z^{-1})r\sin\phi_y, \\
M(5) &= \frac{r}{2}(z+z^{-1}), \\
M(6) &= -\frac{r}{2}(z-z^{-1}), \\
M(7) &= r\cos\phi_y, \\
M(8) &= -ir\sin\phi_y, \\
M(9) &= \frac{r}{2}(z+z^{-1}+2\cos\phi_y)+1.
\end{aligned}
\tag{A8}
$$

[1] See for an extensive review, *Mathematical Physics in One Dimension*, edited by E. H. Lieb and D. C. Mattis (Academic, New York, 1966).
[2] R. Landauer, J. Phys.: Condens. Matter **1**, 8099 (1989).
[3] M. Büttiker, Phys. Rev. Lett. **57**, 1761 (1986).
[4] A. Tekman and P. F. Bagwell, Phys. Rev. B **48**, 2553 (1993).
[5] C. Berthod, F. Gagel, and K. Maschke, Phys. Rev. B **50**, 18 299 (1994).
[6] A. Khater, N. Auby, and D. Kechrakos, J. Phys.: Condens. Matter **4**, 3743 (1992); A. Khater and W. Czaja, Physica B **167**, 33 (1990).
[7] A. Fellay, F. Gagel, K. Maschke, A. Virlouvet, and A. Khater, Phys. Rev. B **55**, 1707 (1997).
[8] J. E. Black and P. Bopp, Surf. Sci. **140**, 275 (1984).
[9] P. Knipp, Phys. Rev. B **43**, 6908 (1991).
[10] A. Lock, J. P. Toennics, and G. Witte, J. Electron Spectrosc. Relat. Phenom. **54/55**, 309 (1990).
[11] Y. Pennec and A. Khater, Surf. Sci. Lett. **348**, L82 (1996).
[12] G. M. Watson, D. Gibbs, and D. M. Zehner, Phys. Rev. Lett. **71**, 3166 (1993).
[13] A. Kara, C. S. Jayanthi, S. Y. Wu, and F. Ercolessi, Phys. Rev. Lett. **72**, 2223 (1994).
[14] E. J. Mele and M. V. Pykhtin, Phys. Rev. Lett. **75**, 3878 (1995).
[15] Z.-J. Tian and J. E. Black, Surf. Sci. **303**, 395 (1994).
[16] A. Virlouvet, H. Grimech, A. Khater, Y. Pennec, and K. Maschke, J. Phys.: Condens. Matter **8**, 7589 (1996).
[17] J. Szeftel and A. Khater, J. Phys. C **20**, 4725 (1987).
[18] A. A. Maradudin, R. F. Wallis, and L. Dobrzynski, *Handbook of Surfaces and Interfaces* (Garland, New York, 1980), Vol. 3.
[19] H. Grimech and A. Khater, Surf. Sci. **323**, 198 (1995).